

Calving of large tabular icebergs from ice shelf rift systems

Ian Joughin^{1,2} and Douglas R. MacAyeal³

Received 9 July 2004; revised 8 October 2004; accepted 2 December 2004; published 21 January 2005.

[1] We used Interferometric Synthetic Aperture Radar to study the detachment process that allowed two large icebergs to calve from the Ross Ice Shelf, Antarctica. Time series of rift geometries indicate that rift widths increased steadily, whereas rift lengths increased episodically through several discrete rift-tip propagation events. We also conducted modeling experiments constrained by the observed rift geometry. Both the observations and model suggest that rift opening, and, thus, tabular-iceberg calving, are largely driven by “glaciological” stresses—stress introduced by the effect of gravity on the ice shelf—rather than by stress introduced by the ocean and atmosphere, e.g., tides and storms. This style of rift propagation is expected to determine the steady, background calving rate of ice shelves and, thus, differs significantly from styles that led to the recent disintegration of ice shelves in response to climate warming, e.g., the Larsen B Ice Shelf on the Antarctic Peninsula. **Citation:** Joughin, I., and D. R. MacAyeal (2005), Calving of large tabular icebergs from ice shelf rift systems, *Geophys. Res. Lett.*, 32, L02501, doi:10.1029/2004GL020978.

[2] Glaciers and ice sheets flow continuously and at relatively steady rates, so the nearly instantaneous calving of Massachusetts-sized icebergs from Texas-sized ice shelves merits attention. Over the 4-year period from 1998–2002, the Filchner-Ronne and Ross ice shelves calved six large icebergs with a combined area of >37,000 km² [Lazzara *et al.*, 1999]. Since iceberg calving balances most of the mass the Antarctic Ice Sheet gains annually via snow accumulation, understanding the mechanisms and controls on the calving process is critical to predicting future ice sheet/shelf behaviour.

[3] Unlike small ice shelves along the Antarctic Peninsula, such as the Larsen B Ice Shelf where melt-related phenomena [Scambos *et al.*, 2000] are the likely cause of its recent disintegration [Rott *et al.*, 1996], the larger Ross and Filchner-Ronne ice shelves lie farther south, in colder environments with little surface melting. These ice shelves calve massive tabular icebergs along detachment boundaries formed by long (>100 km), actively opening rift systems that penetrate the full thickness of the ice shelf, from surface to base. (We distinguish a rift from a crevasse by this degree of penetration.) Although the role these rifts play in calving is well established, i.e., iceberg boundaries are the sides of

rifts, the forces driving rift growth and propagation have yet to be fully understood [Lazzara *et al.*, 1999; van der Veen, 2002]. There are several potential contributors to rift opening. Some are external, including oceanographic (e.g., frictional stress introduced by tidal currents) or atmospheric (e.g., wind stress) forcings. There also are the internal glaciological stresses that govern the creep spreading of ice shelves. Thus, a first step in improving the understanding of large tabular iceberg calving is the determination of the dominant forces that control rift opening and propagation.

[4] Weather satellites and other instruments with frequent coverage have aided in the detection of iceberg calving. The resolution of these instruments is not suited, however, to measuring rift-growth rates leading to calving events. With its high-resolution, all weather and day/night capability, Synthetic Aperture Radar (SAR) is an ideal instrument for studying rift growth. Interferometric SAR (InSAR) is particularly useful for measuring rift opening. Conventional phase-based InSAR provides cm-scale accuracy and speckle-tracking-based InSAR yields errors ranging from about 30 to 80 cm. This study relies on a combination of both methods [Joughin, 2002].

[5] We determined rift-opening rates prior to the calving of two large icebergs, B15 and C19, which calved from the front of the Ross Ice Shelf (Figure 1). Prior to calving, the ice shelf front had reached a position comparable to, or north of, the historical seaward limit [Keys *et al.*, 1998].

[6] Figure 2 shows ice shelf speeds acquired at the onset of the Austral springs of 1997, 2000, and 2001. All three images reveal a strong east-west velocity gradient, which comprises the shear zone where the floating ice shelf is in contact with the grounded ice of Roosevelt Island. The earlier image shows the areas that later calved in March and April 2000 to produce icebergs B15 and B17 [Lazzara *et al.*, 1999]. The large rift along which B15 detached is visible in the 1997 SAR image (Figure 2, brightness) and as a strong discontinuity in speed (Figure 2, color) across much of its length. Just seaward of the eastern rift tip, there is a second smaller rift along which the velocity discontinuity continues. A narrow band of ice separates this pair of rifts, reducing the mechanical coupling of the future B15 to the rest of the shelf near Roosevelt Island. This narrow attachment allowed the entire B15 area to move at nearly a fixed speed, comparable to that nearer the ice front center (~1000 m/yr) where it was firmly attached. In contrast, on the rift's southern edge, the motion conforms to the shear-zone imposed velocity gradient, resulting in an opening rate of nearly 600 m/yr across the rift's eastern edge. As the opening progressed, concentration of stresses at the western rift tip ultimately forced westward rift propagation, eventually giving rise to B15 when the tip intersected another rift perpendicular to the ice front.

[7] Another large rift (rift A) that may yield the next B15-sized iceberg from this region is visible in all three images

¹Jet Propulsion Laboratory, California Institute of Technology, Pasadena, California, USA.

²Now at Polar Science Center, Applied Physics Lab, University of Washington, Seattle, Washington, USA.

³Department of Geophysical Sciences, University of Chicago, Chicago, Illinois, USA.

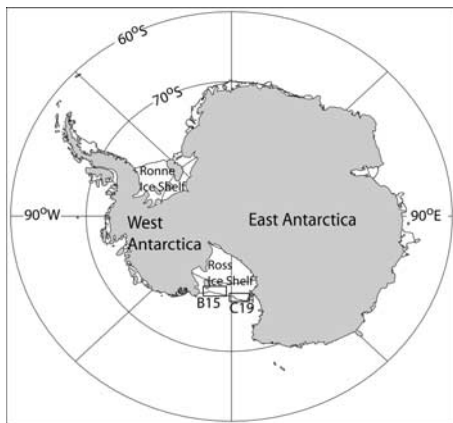


Figure 1. Map showing the location of the Ross Ice Shelf. The box marked B15 corresponds to the area shown in Figure 2 and the box marked C19 to the area shown in Figure 3.

landward of the B15 rift. The SAR imagery indicates that this rift lengthened from 134 km in 1997 to 151 km in 2000. A second 24-km long rift (rift B) also formed over this 3-year period and then expanded an additional 10 km from 2000 to 2001. This pair of rifts is similar to the pair that yielded the weak coupling that led to B15's formation. In September 2001, the maximum opening rate was ~ 250 m/yr across rift B and ~ 150 m/yr across rift A, so that at this stage the rates are only about one third to one half of those preceding the B15 calving.

[8] A black circle (Figure 2) marks an area seaward of Roosevelt Island, which, except for a small area on the future B15, moved relatively slowly in 1997. After the B15 and B17 calvings, however, the peak speed for this region increased to 870 m/yr in September 2000 and to nearly 1050 m/yr by September 2001, leading to 300 to 400 m/yr rift opening rates in 2001. The B17 calving may partially be responsible for the increase, since the pre-B17 area appears to have restrained flow in this area (see Figure 2 (top)). The circled area lies in a heavily rifted region that, although weakened, still supports stress across the shear zone to restrain the future iceberg's eastern margin. The opening rates suggest that the largest block in this region will calve as a small iceberg within the next few years. Optical imagery (http://nsidc.org/data/iceshelves_images/ross.html) indicates that calving of the first block from this region was well underway in January 2004. Once calving removes this and similar smaller blocks, much of the lateral restraint across the shear zone should be removed, leaving the narrow band of ice separated by rifts A and B as the sole attachment to the shelf for the eastern edge of B15's successor. This is almost exactly the same situation as existed prior to the B15 calving (Figure 2 (top)), suggesting that this area of the shelf calves in a fairly regular fashion. We note that the B15 calving also involved a rift perpendicular to the ice front. At present, there are no such rifts present.

[9] Relative to the B15 calving, the case is more complicated for the rift opening and propagation prior to the calving of iceberg C19 in early May 2002. Figure 3a shows the pre-calving velocity for this area. As for B15, a strong velocity discontinuity yielded large rift opening rates

(~ 400 m/yr). Unlike the B15 case, however, the area that eventually calved connects fully across the ice shelf's shear zone. Furthermore, the section that created C19 flowed significantly faster than anywhere else along the shelf front. In contrast, the B15 ice moved "passively" along at roughly the speed of the area where it was strongly connected to the shelf center.

[10] To examine the temporal behaviour of the rift opening, Figure 4 shows velocity profiles across the rift. The thin black lines show 14 individual estimates generated using 24-day interferometric pairs, which were collected during a period with little change in the rift tip position (yellow arrow in Figure 3a). The main ice shelf flows at a nearly a constant speed, but on the C19 area there is temporal variability with maximum differences of up to ± 100 m/yr. These velocities were computed using 24-day image pairs, so the corresponding 24-day displacement variability is ± 6.7 meters. After B15 calved, it grounded itself near C19, where its position fluctuated diurnally by ~ 300 meters (unpublished GPS data) in response to tidally induced tilts on the ocean surface. Therefore, similar tidal effects, which likely have a smaller effect on ice still attached to the shelf, probably drive the variability visible in the Figure 4.

[11] The Figure 4 profiles show flow-speed changes in response to increasing rift length as fracture events drove the rift tip's westward progression. Between April and September 2001, the rift expanded by 3 km in length, increasing the rift-opening rate from 460 m/yr (orange curve) to 520 m/yr (red curve) based on averages of several

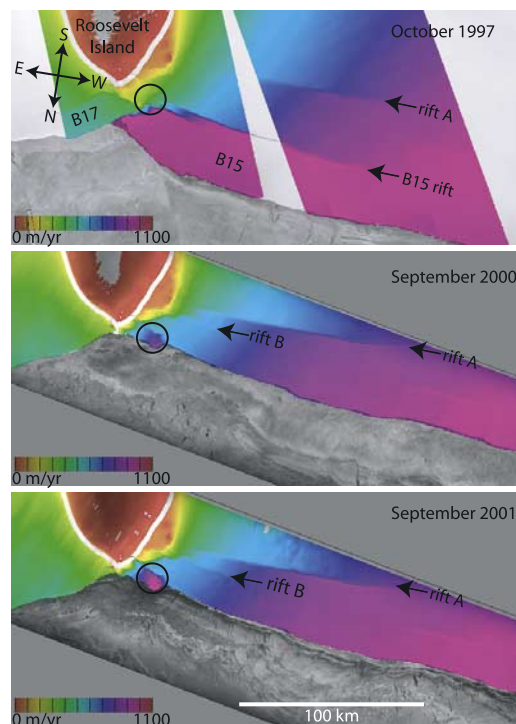


Figure 2. Ice flow speed (color) and SAR amplitude (brightness) along the eastern side of the Ross Ice Shelf in October 1997, and September 2000 and 2001. Ice flow velocity was computed using InSAR phase and speckle tracking [Joughin, 2002] with corrections for tidal displacements [Padman *et al.*, 2003].

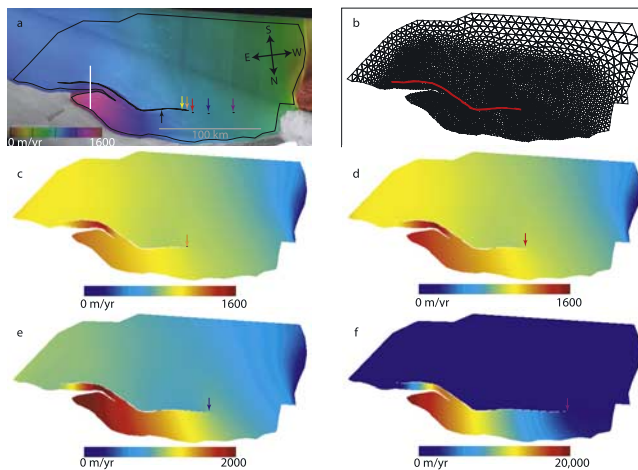


Figure 3. Results for Iceberg C19 showing a) estimated velocity (color) and SAR image (brightness) and rift tip locations (arrows), b) finite element mesh used in modeling. Model results were calculated for the western rift tip at locations from c) September 25, 2000, through April 29, 2001 (orange arrow), d) September 20, 2001 through March 7, 2002 (red arrow), e) March 31 through April 24, 2002 (blue arrow), and on f) May 2, 2002 (purple arrow). Rift tip locations were unmonitored during the months of May through August when the winter eclipse period prevented RADARSAT from collecting data at extreme southern latitudes. The yellow arrow indicates the rift tip location in October 2002, and the Figure 4 caption describes the black arrow. We averaged results from 14 interferometric pairs collected over the period from September 2000 to April 2001 to produce the velocity estimate. The thick white line shows the location of the profile plotted in Figure 4.

estimates. A much larger fracture event, or series of fracture events, occurred in March 2002 that lengthened the rift by 18 km and increased the rift-opening rate to 630 m/yr. Just prior to calving, between April 24 and May 2, 2002, the rift lengthened by another 24 km, substantially increasing the rift-opening rate (purple curve, Figure 4). Because the image pair used to generate this curve spans the interval from April 8 to May 2, 2003, the data records displacement from both before and after the rift growth. If we assume the rift expansion occurred on April 24, then a lower bound on the opening rate is 1967 m/yr. Alternatively, if the rift expanded exactly 1 day before May 2, then the opening rate would be $\sim 11,000$ m/yr.

[12] The observations alone do not rule out oceanographic and atmospheric causes, which are likely to be episodic. The steady opening between rift propagation events, however, suggests that glaciological stresses are a major driver in tabular iceberg calving. To test this hypothesis, we experimented with a finite-element ice shelf model [MacAyeal *et al.*, 1996] to see if we could reproduce the rift opening behavior observed prior to the C19 calving. Figure 3b shows the finite-element mesh and model domain with the first experiment's rift location. We applied an open-water boundary condition within the rift and at the ice shelf front and applied a kinematic (velocity) boundary condition along the remaining boundary of the modeled ice shelf domain.

[13] We performed four experiments with the western rift tip located at the orange, red, blue, and purple locations shown in Figure 3, which follow the observed sequence of rift growth. The first experiment (Figure 3c) modeled the rift at its minimum observed position (Figure 3a). This yielded a 238-m/yr opening rate, which is just over half the observed rate. The narrow band of ice along the rift's eastern seaward edge moves faster than the other areas, which is unlike the observed case, where the main body of ice that formed C19 moved the fastest. In the second experiment, we lengthened the rift by 3 km (Figure 3d). This increased the opening rate to 334 m/yr compared to the observed rate of 520 m/yr. For the third case, we expanded the modeled rift by 18 km (Figure 3e). This increased the rift-opening rate to 971 m/yr, which exceeds the observed rate of 630 m/yr. Finally, at the rift's final observed length (Figure 3f), the model yielded an opening rate of 16,400 m/yr, which is consistent with the observations if the rift's final expansion occurred within ~ 24 hours of the May 2 image acquisition.

[14] Qualitatively, the model mirrors the observations: modeled glaciological stresses lead to opening rates that accelerate with rift expansion. Quantitatively, the results are not so close, with the first two experiments yielding opening rates $\sim 50\%$ less than observed and the third experiment $\sim 50\%$ larger. There are several potential causes for this mismatch. Ice shelf flow is largely driven by thickness gradients, and the quality of the thickness data used in the model was relatively poor for this section of the ice shelf [Lythe *et al.*, 2001]. Furthermore, the thickness data were acquired several years before the velocity and image data, resulting in ice-motion-induced several-kilometer registration errors. Another factor may be that the rift is filled with a mélange of sea and glacial ice with unknown mechanical properties [Rignot and MacAyeal, 1998], which may affect the force balance within the rift [Larour *et al.*, 2004, 2005; J. N. Bassis *et al.*, Episodic propagation of a rift on the Amery Ice Shelf, East Antarctica, submitted to *Geophysical*

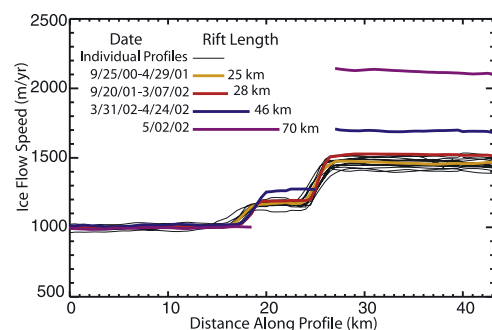


Figure 4. Plots of ice flow speed along the profile at the location shown in Figure 4a. These plots show the difference in speed across the rift that causes it to widen. The 14 individual profiles were generated from data collected over the period from September 2000 to April 2001. The orange curve is the average of the 14 individual profiles and the red curve is the average of 6 interferometric pairs. The blue and purple curves are from single interferometric pairs. The relative lengths of the western section of the rift were measured relative to the black arrow shown in Figure 3.

Research Letters, 2004]. We ignored this mélange, modeling the rift as a single, narrow crack. In addition, we can only infer the rift location from its surface expression in the SAR imagery, so we assumed that the rift penetrates the full ice thickness wherever it was visible on the surface, which may not be the case.

[15] Despite the model's deficiencies, the qualitative agreement between the model and observations argues that glaciological stresses are the major control on rift opening, since the model excludes other potential causes. This is consistent with similar findings for the Ronne Ice Shelf [Larour *et al.*, 2004, 2005]. The observations of steadily opening rifts on the eastern and western sides of the shelf front also support this conclusion. Steady rift propagation rates over a 5-year period were observed for a smaller rift system on Amery Ice Shelf, with a possible seasonal trend superimposed, which may suggest other processes [Fricker *et al.*, 2005]. The images we analyzed, however, did not reveal any apparent seasonal trend on the Ross Ice Shelf.

[16] That internal ice shelf processes appear to dominate the calving processes—at least for large tabular icebergs—offers an avenue to incorporate the calving process into fully coupled ice sheet/shelf models in an empirical manner. This is important since present-day calving rates and their relationship to ice sheet stability under differing climate conditions likely will be studied best within the context of numerical ice sheet/ice shelf simulations.

[17] **Acknowledgments.** I.J. performed his contribution to this work at the Jet Propulsion Laboratory, California Institute of Technology, under contract with NASA. D.R.M. was supported by the National Science Foundation under grant NSF OPP-0229546. The RADARSAT data were acquired by the Canadian Space Agency and were processed to L0-products by the Alaska SAR Facility. Mosaicked RADARSAT SAR amplitude images were provided by K. Jezek of the Byrd Polar Research Center. D. G. Vaughan and the BEDMAP project produced the ice thickness data set. Comments by an anonymous reviewer and associate editor significantly improved this manuscript.

References

- Fricker, H. A., N. W. Young, R. Coleman, J. N. Bassis, and J.-B. Minster (2005), Multi-year monitoring of rift propagation on the Amery Ice Shelf, East Antarctica, *Geophys. Res. Lett.*, *32*, L02502, doi:10.1029/2004GL021036.
- Joughin, I. (2002), Ice-sheet velocity mapping: A combined interferometric and speckle-tracking approach, *Ann. Glaciol.*, *34*, 195–201.
- Keys, H. J. R., S. S. Jacobs, and L. W. Brigham (1998), Continued northward expansion of the Ross Ice Shelf, Antarctica, *Ann. Glaciol.*, *27*, 93–98.
- Larour, E., E. Rignot, and D. Aubry (2004), Modelling of rift propagation on Ronne Ice Shelf, Antarctica, and sensitivity to climate change, *Geophys. Res. Lett.*, *31*, L16404, doi:10.1029/2004GL020077.
- Larour, E., E. Rignot, and D. Aubry (2005), Processes involved in the propagation of rifts near Hemmen Ice Rise in the Ronne Ice Shelf, Antarctica, *J. Glaciol.*, in press.
- Lazzara, M. A., K. C. Jezek, T. A. Scambos, D. R. MacAyeal, and C. J. van der Veen (1999), On the recent calving of icebergs from the Ross Ice Shelf, *Polar Geogr.*, *23*, 201–212.
- Lythe, M. B., D. G. Vaughan, and the BEDMAP Consortium (2001), BEDMAP: A new ice thickness and subglacial topographic model of Antarctica, *J. Geophys. Res.*, *106*, 11,335–11,351.
- MacAyeal, D. R., V. Rommelaere, P. Huybrechts, C. L. Hulbe, J. Determann, and C. Ritz (1996), An ice shelf model test based on the Ross Ice Shelf, Antarctica, *Ann. Glaciol.*, *23*, 46–51.
- Padman, L., S. Erofeeva, and I. Joughin (2003), Tides of the Ross Sea and Ross Ice Shelf cavity, *Antarct. Sci.*, *15*, 31–40.
- Rignot, E., and D. R. MacAyeal (1998), Ice shelf dynamics near the front of the Filchner-Ronne Ice Shelf, Antarctica, revealed by SAR interferometry, *J. Glaciol.*, *44*, 405–418.
- Rott, H., P. Skvarca, and T. Nagler (1996), Rapid collapse of northern Larsen Ice Shelf, Antarctica, *Science*, *271*, 788–792.
- Scambos, T. A., C. Hulbe, M. Fahnestock, and J. Bohlander (2000), The link between climate warming and break-up of ice shelves in the Antarctic Peninsula, *J. Glaciol.*, *46*, 516–530.
- van der Veen, C. J. (2002), Calving glaciers, *Prog. Phys. Geogr.*, *26*, 96–122.
- I. Joughin, University of Washington, 1013 NE 40th Street, Seattle, WA, 98105-6698, USA. (ian@apl.washington.edu)
- D. R. MacAyeal, Department of Geophysical Sciences, University of Chicago, 5734 S. Ellis Ave., Chicago, IL 60637, USA. (drm7@midway.uchicago.edu)